



A PARAMETRIC STUDY ON THE PERFORMANCE OF MASONRY-INFILLED RC FRAME STRUCTURES

Xiaomin Wang⁽¹⁾, Maosheng Gong⁽²⁾, Ruishan Li⁽³⁾, Zhanxuan Zuo⁽⁴⁾, Baofeng Zhou⁽⁵⁾

⁽¹⁾ Research Assistant, Key Laboratory of Earthquake Engineering and Engineering Vibration; Institute of Engineering Mechanics, China Earthquake Administration, Harbin, 150080, China, E-mail: wxmrm@foxmail.com

⁽²⁾ Professor, Key Laboratory of Earthquake Engineering and Engineering Vibration; Institute of Engineering Mechanics, China Earthquake Administration, Harbin, 150080, China, E-mail: gmsheim@163.com

⁽³⁾ Research Assistant, Key Laboratory of Earthquake Engineering and Engineering Vibration; Institute of Engineering Mechanics, China Earthquake Administration, Harbin, 150080, China, E-mail: lrshan22@hotmail.com

⁽⁴⁾ Research Assistant, Key Laboratory of Earthquake Engineering and Engineering Vibration; Institute of Engineering Mechanics, China Earthquake Administration, Harbin, 150080, China, E-mail: zuo-zhanxuan@sina.com

⁽⁵⁾ Associate Professor, Key Laboratory of Earthquake Engineering and Engineering Vibration; Institute of Engineering Mechanics, China Earthquake Administration, Harbin, 150080, China, E-mail: zbf166@126.com

Abstract

Masonry-infilled reinforced concrete (RC) frame structures, as one of the most common forms of building constructions, have been built in many parts of the world. The evaluation of the seismic performance of masonry infilled RC frame structures is a challenging work that has not yet been resolved despite the numerous efforts have been invested in the last decades. The main challenge is because of the complexity of interaction between the infill and the frame, which is affected by the geometry, applied vertical load, reinforcement details, and some other factors. In this paper, a finite element modeling, which adopts an improved extended finite element method (XFEM) to model the concrete in the RC frame members as well as masonry units in the infill panels, and employs discrete interface elements to model the behavior of mortar joints between masonry units and the behavior of the frame-to-infill interface, is proposed to simulate the performance of masonry-infilled RC frames. The effectiveness of the proposed modeling is validated by analyzing several masonry-infilled RC frame specimens. With the validated finite element modeling, a parametric study has been systematically conducted to consider the effect of different geometrical dimensions, design parameters and material properties on the behavior of masonry-infilled RC frames, which concerns aspect ratio of infill panel, vertical load applied on the specimen, the distribution of the vertical load between column and beam, longitudinal reinforcement and transverse reinforcement of columns, sectional dimensions of columns, thickness of the infill panel, frictional coefficient of mortar joints, and height of beam section. The analytical results reveal the influence extent and general tendency of these parameters on the structural bearing capacity and failure patterns, and the interaction mechanism between the infill and the bounding frame under the lateral load. The parametric study result will provide a data support to develop a simplified procedure for the lateral load-lateral displacement relation of masonry-infilled RC frame structures.

Keywords: masonry-infilled RC frame structures, finite element modeling, XFEM, interface elements, parametric study



1. Introduction

Masonry-infilled reinforced concrete (RC) frame structures are widely built in many parts of the world. The infill walls are frequently used as interior partitions and exterior walls in buildings for architectural needs or aesthetic reasons. In structural design, the infill walls are often treated as nonstructural elements and their effect is omitted in the analysis models. However, the infill walls have significant contribution to the seismic performance of RC structures, which can highly increase the strength and stiffness and affect the failure pattern of structures, either in a positive or negative way.

Significant researches have been reported in a large number of literatures to attempt to understand the behavior of masonry-infilled RC frame structures. Early researches primarily adopt experimental methods to investigate the behavior and damage phenomenon of infilled frame structures. Fiorato et al.[1] performed 27 of quasi-static tests on 1/8-scale infilled RC frames under monotonic loading, considering the effects of the number of stories and spans, axial load, and infill wall openings. Klingner and Bertero[2] performed a shaking test on the bottom 3.5 floors of an 11-storey building, and examined the effect of various types of infill walls on hysteretic performance. Zarnic and Tomazevic[3] performed cyclic loading tests on 28 of infilled frame specimens, considering the effects of filling materials, reinforcements in the infill wall and openings on hysteretic performance. Furthermore, the effect of different strengthening technologies is studied. Mehrabi et al.[4] conducted 14 of tests on 1/2-scale infilled RC frames under monotonic and cyclic loadings, and studied the effects of loading history, aspect ratio, and vertical load distribution. Mosalam et al.[5] conducted the quasi-static tests on 1/4-scale single-story infilled steel frames, and studied the effect of the relative strength between the frame and the infill wall and the infill wall openings on structural performance. Al-Chaar et al.[6] tested 5 of 1/2 scale single-story infilled RC frames with different spans and filling materials, and pointed out the failure mechanism of the infilled frames is determined by shear strength, compressive strength, lateral stiffness, geometric dimension and other factors. Anil and Altin[7] performed cyclic loading tests on 9 of 1/3-scale single-story single-span partially infilled RC frames, and studied the effect of aspect ratio, opening position, and frame-infill connections on the strength, stiffness and energy dissipation of the structure. Blackard et al.[8] and Stavridis[9] performed a series of cyclic loading tests on 2/3 scale single-story single-span infilled non-ductile RC frames. Based on the same prototype structure, Stavridis[9] conducted shaking table tests on a 2/3 scale three-story two-span infilled RC frame.

The uncertainty of the interaction between the infill and bounding frame affects the behavior and damage of infilled RC frames, which may produce different failure patterns and is affected by a lot of factors. However, due to many practical considerations, the number of test specimens is generally limited when conducting an experimental research on infilled RC frames, and it is difficult to comprehensively consider the effect of various factors on structural performance. Moreover, for a specific factor, it is difficult to perform too many tests to accurately discuss the effect law of this parameter. In addition, for some structural design parameters, such as the geometric form, arrangement of reinforcements, and distribution of vertical loads, it is difficult to change the value of these parameters due to implementation restriction. Therefore, it is an alternative method to use an accurate numerical model to perform the parameter analysis, and it is of great significance to understand the performance of infilled RC frame structures. Following a series of work by Shing[4,9,10], the authors have proposed a XFEM-based finite element modeling[11], which combines an improved XFEM with interface elements to simulate the behavior and possible failure patterns of masonry-infilled RC frames. With this modeling, a parametric study is systematically performed, the influence extent and general tendency of various parameters are discussed in details. The analysis result will provide a strong data support for developing a simplified analysis procedure of infilled RC frame structures.

2. Finite Element Modeling

2.1 Discretization scheme

Fig. 1 illustrates the discretization scheme of the proposed modeling for a one-story one-bay infilled frame specimen. In this scheme, the XFEM is used to model the cracking behavior and compressive failure of



concrete in RC frame members and masonry units in infill panels, employing two-dimensional plane stress 4-node quadrilateral elements. It should be mentioned that multiple continuous cracks are allowed in this model. Reinforcing bars in concrete members are modeled using 1-D truss elements with an elastic-hardening-plastic constitutive model. The hardening modulus is assumed to be 1.0% of the elastic modulus. The von Mises yield surface with a total stress range of twice the yield stress (Bauschinger effect) is adopted.

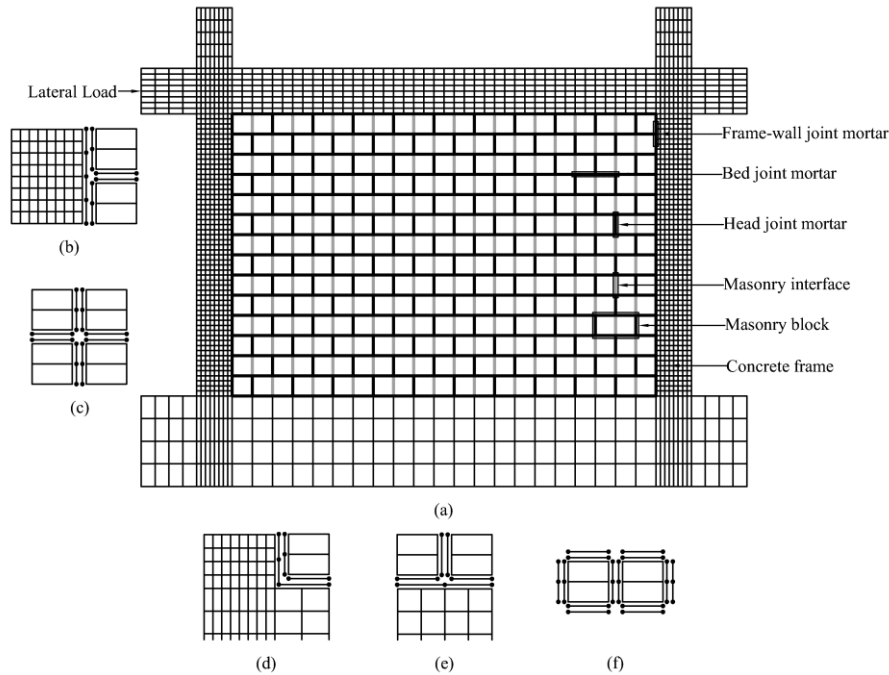


Fig. 1 Finite-element modeling for masonry-infilled RC frame: (a) discretization scheme; (b–e) detailed information for the connectivity of interface elements; (f) discretization scheme of masonry units

In infill panels, the mortar joints between masonry units and the joints at frame-to-infill interface are represented by zero-width interface elements. The possible tensile splitting cracks in masonry units are also introduced by interface elements. The detailed information for the connectivity of interface elements is displayed in Fig. 1(b)–(e). The discretization scheme of masonry units is illustrated in Fig. 1(f), in which each masonry unit is modeled by 2×2 4-node quadrilateral elements that are inter-connected with two vertical interface elements. Since interface elements in the model are usually zero width with no thickness, the dimensions of masonry units are modified to maintain the same overall dimensions of a masonry-mortar assembly. In addition, the mesh generation of RC frame members depends on the dimension of masonry elements, since the frame-to-infill joints are modeled by interface elements.

2.2 Numerical verification

Two of 1/2 scale one-story one-bay masonry-infilled RC frame specimens, namely specimens 8 and 9 in the test[4], are analyzed to verify the capability of the proposed finite element modeling. Specimens 8 and 9 are infilled with weak and strong walls, respectively. The design details of test specimens includes the dimension of the frame, beam and column sections and reinforcement arrangement can be found in Mehrabi et al.[4]. In the analysis, the vertical load is firstly applied refer to the loading scheme in the experiment. Then, the analysis is pursued by applying monotonically increased lateral displacement at the left side of the beam. The detailed description for the modeling can be found in Zhai et al.[11].

Fig. 2 and 3 compare lateral load-lateral displacement curves between finite element analyses and experimental results for specimens 8 and 9, respectively. It is concluded that a pretty good agreement between the numerical and experimental results is achieved, with the initial stiffness, peak lateral strength, and post-peak response captured very well.

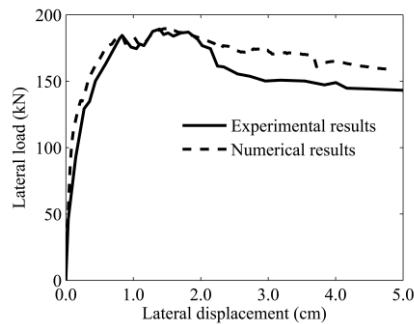


Fig. 2 Lateral load-lateral displacement curves for specimen 8

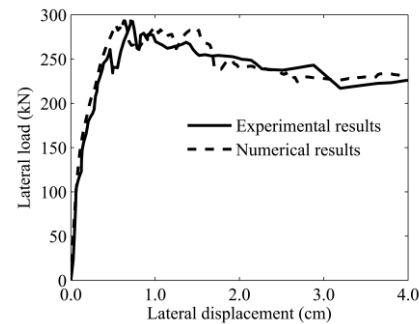


Fig. 3 Lateral load-lateral displacement curves for specimen 9

Next, the failure patterns for specimens 8 and 9 are discussed. Fig. 4 displays the failure patterns of specimen 8 obtained from the numerical analysis at two different lateral displacements and the final state of experimental result, respectively. It should be mentioned that the deformations for two lateral displacements are magnified with different factors to better reflect the failure behavior of frame specimens. An overall observation has shown that a good match between numerical and experimental results is achieved. For specimen 9, the failure patterns of numerical result at two different lateral displacements and the final failure pattern of test result are shown in Fig. 5. A good agreement is also achieved from a macroscopic view by comparing these two results.

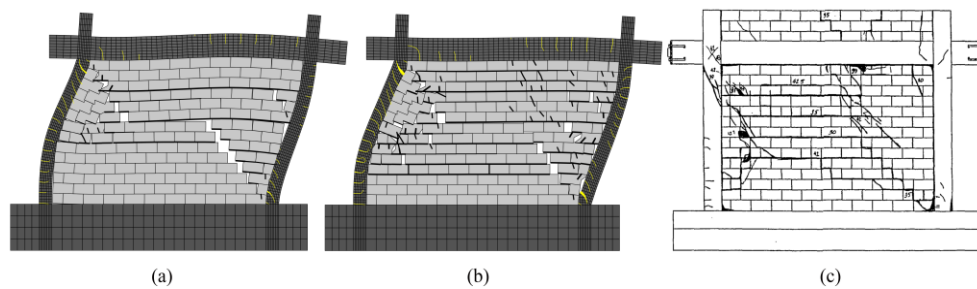


Fig. 4 Numerical and experimental failure patterns for specimen 8 at different lateral displacements

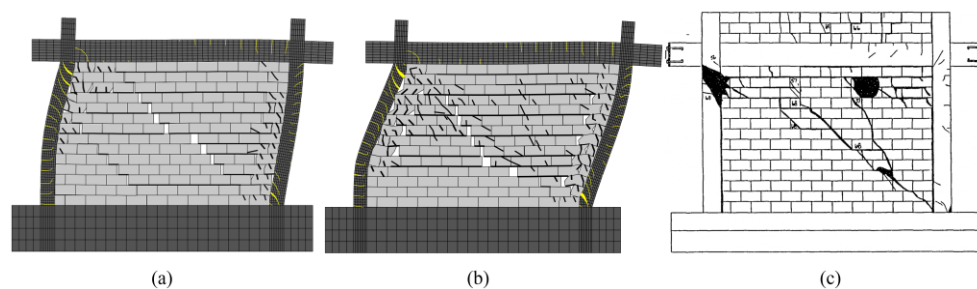


Fig. 5 Numerical and experimental failure patterns for specimen 9 at different lateral displacements

3. Parametric Study

In this section, specimen 9 is adopted as the basic model, named SP9. The parameters examined in this paper mainly include: aspect ratio of infill walls, applied vertical load and its distribution between the beam and columns, longitudinal reinforcement and transverse reinforcement of frame columns, column section dimension, thickness of infill walls, frictional coefficient of mortar joints, and the height of beam section. In each numerical simulation, only one of these parameters is changed and the other parameters remain constant, which facilitates the discussion of the effect of different parameters and obtains the importance information of the parameters.



3.1 Effect of aspect ratio of infill wall

In model SP9, aspect ratio (height-to-width) of the infill wall is 0.67. In order to investigate the effect of aspect ratio of the infill wall, three additional infilled RC frame models with different geometric forms by keeping height of frame unchanged and adjusting frame span are analyzed in this section. This is mainly due to the fact that the story height of structure is generally fixed in a building, or the range of change is small, while the range of span is usually large. Three models are named AR.82, AR.56 and AR.48 according to aspect ratio of the infill wall.

The lateral load-lateral displacement curves of models AR.82, SP9, AR.56, and AR.48 are shown in Fig. 6. In general, there are obvious differences in terms of initial stiffness, peak load, and corresponding lateral displacement at peak load. As the span of the infill wall increases, the stiffness and load capacity of structure correspondingly increase. Moreover, the lateral displacement corresponding to peak load gradually decreases with the increase of span of the infill wall.

Fig. 7 shows failure patterns of the infilled frames under different aspect ratios when the lateral displacement reaches 2.0cm (the same as the displacement shown in Fig. 5(a)). In model AR.82, due to small span of frame, a diagonal compression strut path is formed in the infill wall. In addition, the overturning moment of frame under lateral load results in an axial tensile force in the windward column. Due to smaller span, the shear capacity of windward column is slightly reduced under the axial tensile force. At the same time, larger bending moment also results in higher axial pressure at the bottom of leeward column. Therefore, compared with other models, the compressive stress in the infill wall and leeward column of this model is relatively high, which increases the shear capacity of leeward column and the filled wall. In models AR.56 and AR.48, a penetrating crack that combines the stepped diagonal crack with the shear slip is formed in the infill wall, which is similar to the damage of model SP9. With the increase of lateral displacement, the top of windward column and the bottom of leeward column also suffer shear crack damage.

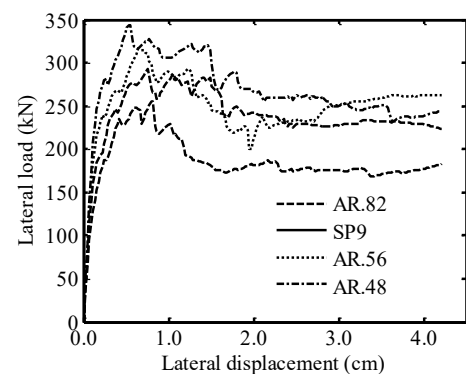


Fig. 6 Lateral load-lateral displacement curves for masonry-infilled RC frame models with different aspect ratios

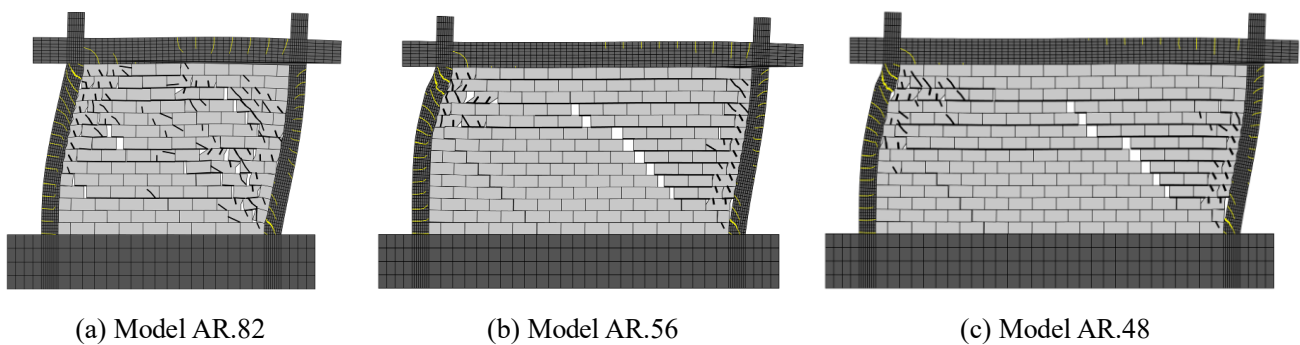


Fig. 7 Failure patterns for masonry-infilled RC frames with different aspect ratios

3.2 Effect of vertical load

The applied vertical load is an important factor affecting the bearing capacity of masonry-infilled RC frame structures. In order to study the effect of vertical load on structural performance, this section establishes 5 numerical models under different vertical loads. In model SP9, the total vertical load was 293.7kN, and 2/3 of the load was applied to two columns and 1/3 of the load to the top of beam. The minimum load considered in this section is the case where no vertical load is applied, and it is named model V0; while other models are named V0.5, V1.5, and V2.0 according to the ratio of the applied load and the load on model SP9.



The lateral load-lateral displacement curves of models V0, V0.5, SP9, V1.5 and V2.0 are plotted in Fig. 8. The initial stiffness in all models is basically the same. However, when the non-linearity of the curve begins to appear, the corresponding lateral loads are significantly different. When the vertical load is larger, the peak lateral load is larger, and the corresponding lateral displacement at the peak load is slightly reduced. This may be because the vertical load on the infill wall restricts the slip of mortar joints. In addition, the difference of the peak load between two adjacent curves is basically the same, and there is a linear relationship between the peak lateral load and the vertical load.

The failure patterns of models V0, V0.5, SP9, V1.5 and V2.0 at the lateral displacement of 2.0cm are shown in Fig. 9. The failure patterns of these models are generally consistent, all forming diagonal shear/slipping cracks in the infill wall and shear failure in columns. However, the damage of infilled walls and frame columns is still significantly affected by vertical loads. The increase of vertical load constrains the upward arching deformation of the infill wall, which causes the damage of the infill wall to gradually shift downward. Meanwhile, the increase of vertical load improves the anti-slipping of mortar joints. Therefore, the diagonal compression damage gradually increases as the increase of vertical load. The constraint of vertical deformation of the infill wall also increases its horizontal deformation, which results in a heavier damage of frame column.

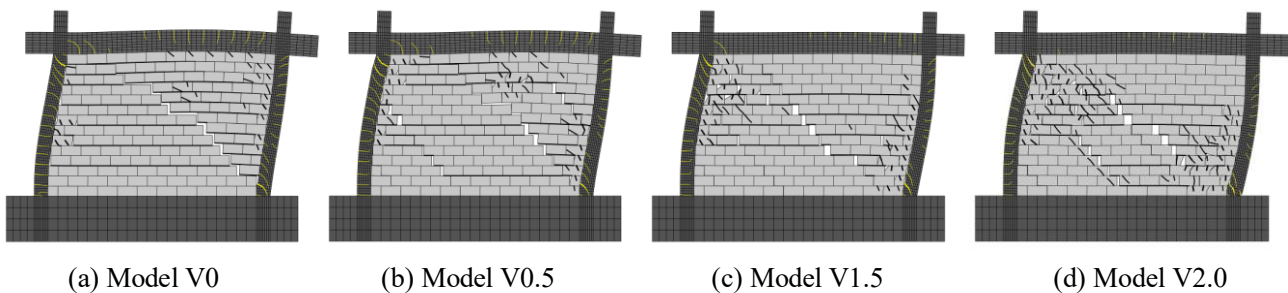


Fig. 9 Failure patterns for masonry-infilled RC frames with different vertical loads

3.3 Effect of vertical load distribution ratio between beam and column

The last section mainly analyzes the effect of vertical load value. In this section, the effect of different vertical load distribution ratio between frame beam and column is studied. Four additional models with different proportions of vertical load between frame columns and beam are analyzed. Each model is defined by the proportion of vertical load applied on beam, and they are named VW0, VW1/2, VW2/3 and VW1, respectively. The lateral load-lateral displacement curves of these models are shown in Fig. 10. The initial stiffness of these models is basically the same. The initial stiffness increases slightly as the load applied on columns increases, which indicates that if total vertical load is unchanged, the load on columns has a greater effect on the stiffness rather than the load on the infill wall; however, this effect is nearly negligible. Once the non-linearity begins to appear, the load capacity of

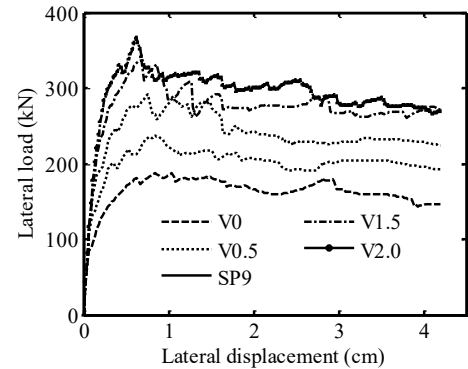


Fig. 8 Lateral load-lateral displacement curves for masonry-infilled RC frame models with different vertical loads

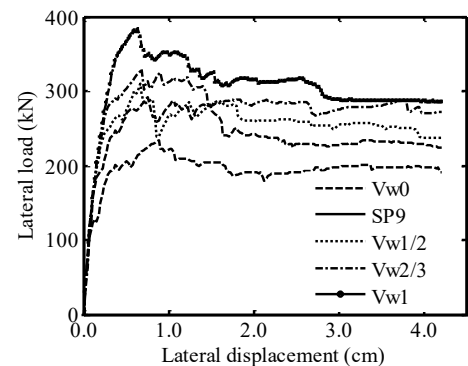


Fig. 10 Lateral load-lateral displacement curves for masonry-infilled RC frame models with different load distribution ratios



curves mainly depends on the vertical load applied on the infill wall. In addition, when the load on beam is larger, the lateral displacement corresponding to the peak load is smaller, which is the same as the phenomenon in the last section.

The failure patterns of the models at the lateral displacement of 2.0 cm are shown in Fig. 11. It can be seen that the failure patterns of these models are similar to that in the last section. The increase of vertical load on beam restrains the vertical deformation of the infill wall, and increases the damage of the lower part in the infill wall, especially in the right lower part. However, compared with the last section, there are still some differences in details. In model VW0, although the vertical load on the infill wall is 0, the vertical load on frame column is large, which enhances the lateral load resistance of frame column. Therefore, the frame has a greater constraint on the infill wall and a compression cracking failure is observed in the infill wall. In addition, the shear failure of frame columns in these models gradually increases as the vertical load ratio on frame beam increases, which is mainly because the axial pressure on columns is gradually decreased, this greatly weakens the shear capacity of columns.

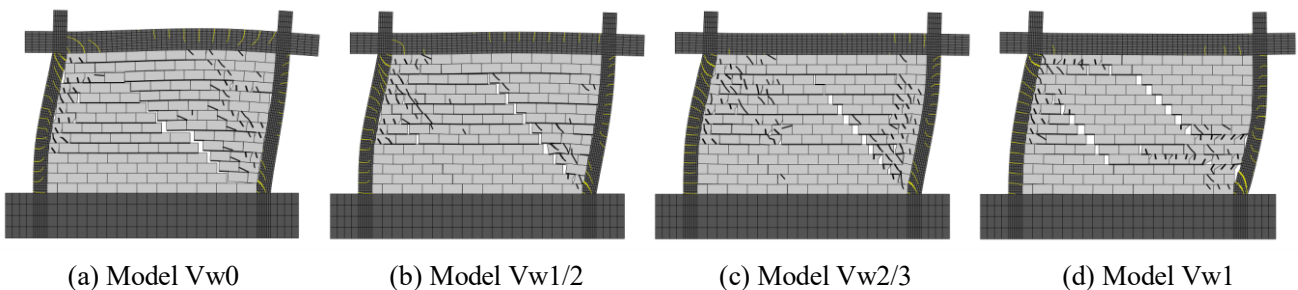


Fig. 11 Failure patterns for masonry-infilled RC frames with different load distribution ratios

3.4 Effect of longitudinal reinforcement

One of the most important components in infilled RC frame structures that determines bearing capacity is frame column, and the bearing capacity of column depends on longitudinal reinforcement, transverse reinforcements, and sectional size of column. Therefore, the following three sections will discuss the influence of these three factors on the performance respectively. In this section, the effect of longitudinal reinforcement of column is firstly studied. Six numerical models with different column reinforcements are analyzed, respectively. According to the ratio of column reinforcement ratio to that of model SP9, these models are named Ro0.5, Ro1.5, Ro2.0, Ro2.5, Ro3.0 and Ro4.0 respectively.

The lateral load-lateral displacement curves of seven models are shown in Fig. 12. It shows that longitudinal reinforcement ratio (LRR) does not substantially affect initial stiffness and lateral load where the non-linearity begins to appear. This may be because these two values mainly depend on the stiffness of columns and infill wall. However, the influence of the reinforcement on it is relatively small. However, the increase of LRR increases the column's bending capacity. Therefore, the peak load of the model is improved. In addition, the increase of LRR improves the ductility of the model. It can be seen that the corresponding lateral displacement at the peak load increases significantly as the increase of LRR. It should be pointed out that a bi-linear constitutive relation is used for the reinforcement in this paper, and the strength decline of the reinforcement is not considered. In the models with really high LRR, the lateral load even continue to rise. This is because of the definition of numerical model, which will not occur in practice. The failure patterns of six models are similar to the failure pattern of model SP9, and

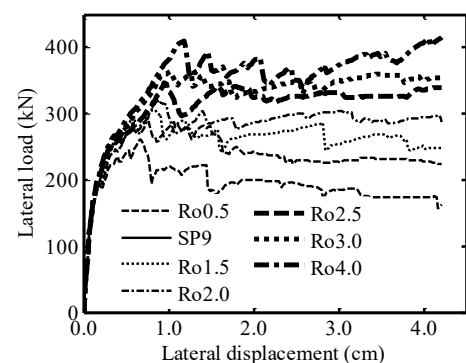


Fig. 12 Lateral load-lateral displacement curves for masonry-infilled RC frame models with different reinforcement ratios in columns



not shown in this section.

3.5 Effect of transverse reinforcement

The effect of transverse reinforcement is analyzed in two ways. Firstly, the area of transverse reinforcement is adjusted. According to the ratio of transverse reinforcement area, these models are named St0.5, St2.0, St3.0 and St4.0. Fig. 13 shows the lateral load-lateral displacement curves. Five models have the same properties in the initial stage, including initial stiffness, yield point, and general growth trend. In addition, these models also have the same peak load. It shows that the increase in the number of transverse reinforcements does not increase the bearing capacity at early stage. However, increasing transverse reinforcements increases the ductility.

The failure patterns of five models are similar and not shown here for conciseness. After the occurrence of cracks in the infill wall, the increase in the number of transverse reinforcements prevents the failure of columns, thereby improving the lateral strength to a certain extent. Eventually, the leeward column reaches its capacity and some inclined cracks occur. Nonetheless, these do not show a brittle load drop in load-displacement curves because transverse reinforcements allow the structure to maintain its resistance. In the windward column, additional transverse reinforcements prevent large inclined cracks appearing, and the column ends up being damaged by bending, which is a more desirable failure mechanism.

This section also examines the effect of transverse reinforcement spacing on structural performance. Two models with twice and half of the transverse reinforcement spacing in model SP9 are analyzed and named models Ds0 and Ds2, respectively. Models Ds0 and Ds2 actually have the same transverse reinforcement area as the models St0.5 and St2.0, but in a different distribution way. Therefore, the lateral load-lateral displacement curves and failure patterns of analyses are not presented. As expected, the influence the amount of transverse reinforcement in two distribution ways tends to be the same. The initial behavior and peak load of all models are not affected, while the ductility is improved as the amount of transverse reinforcement increase. The failure pattern is basically the same for models with the same transverse reinforcement amount.

3.6 Effect of column section

In this section, two sets of analyses are studied to investigate the effect of section height and width of frame columns on structural performance. Firstly, five numerical models are analyzed for the effect of section height. In model SP9, the height of column section is 178 mm. The other models are named Hc153, Hc203, Hc228 and Hc253 according to the height of column section.

The lateral load-lateral displacement curves of five models are shown in Fig. 14. The height of column section has a certain effect on the initial stiffness and lateral load corresponding to the appearance of the non-linearity, but the effect is not large. Meanwhile, the increase of column section height also increases the peak load. However, because the change range of section height is relatively small, the effect of section height on peak load is small too. The corresponding lateral displacements at the peak load are similar, but a slight increase is presented as the peak load increases. In addition,

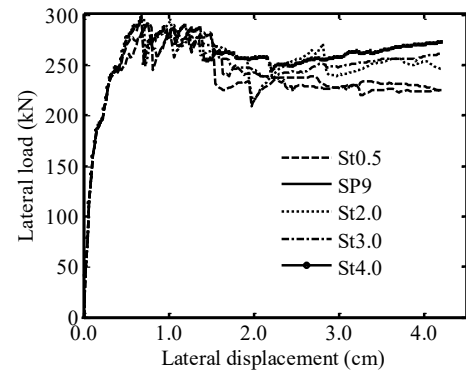


Fig. 13 Lateral load-lateral displacement curves for masonry-infilled RC frame models with different amounts of transverse reinforcement

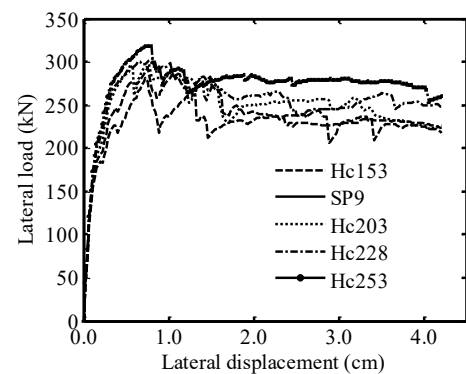


Fig. 14 Lateral load-lateral displacement curves for masonry-infilled RC frame models with different heights of columns



the ductility of the models is not affected.

Fig. 15 shows failure patterns of different models when the lateral displacement is 2.0 cm. With the increase of section height, the bending and shear capacity of columns are both improved, and the damage is gradually concentrated at the top of windward column and the bottom of leeward column. The increase of section height also restricts the deformation of infill wall. The slipping along bed joints gradually decreases, and the compression cracking of the wall gradually increases.

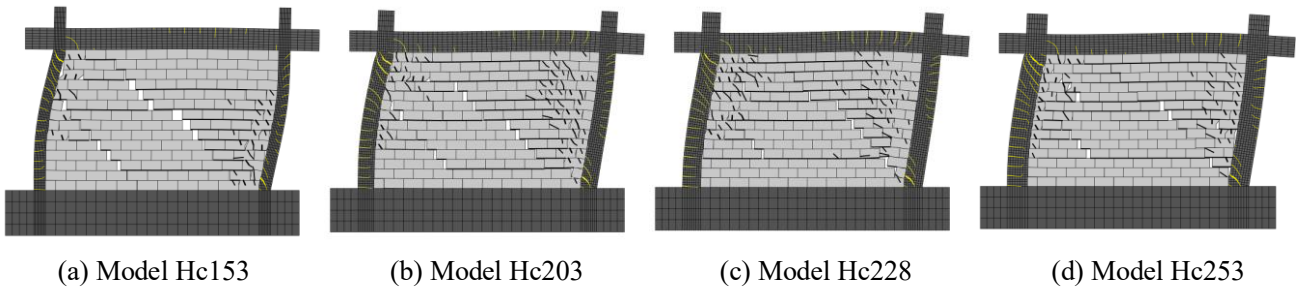


Fig. 15 Failure patterns for masonry-infilled RC frames with different heights of columns

Next, the effect of section width of columns is analyzed. The section width mainly affects the shear strength of columns. Therefore, only two additional models with different column section widths are adopted here, which are named Bc165 and Bc190 respectively. Fig. 16 shows the lateral load-lateral displacement curves of three models. As expected, the width of column section has a very small effect on the early stage behavior. However, it has a slight effect on the ductility of the model. The failure patterns of three models are basically the same, and not shown for conciseness. However, the shear failure at the end of columns is slightly reduced with the increase of section width.

3.7 Effect of thickness of infill wall

The infill wall is another important component that determines the performance of masonry-infilled RC frame structures. The influence of the infill wall on the structural performance has always been an important aspect in the research of infilled RC frame structures. In numerical verification of infilled RC frame specimens, influence of masonry infill wall has been preliminarily discussed. The thickness of the infill wall in model SP9 is 92mm. In this section, four additional models with different thickness of infill walls are analyzed to further study the effect of thickness of the infill wall. According to the thickness of the infill wall, these models are named Wt062, Wt122, Wt152 and Wt182, respectively.

The lateral load-lateral displacement curves of five models are shown in Fig. 17. It can be seen that the increase in the thickness of the infill wall significantly affects the initial stiffness, corresponding lateral load when the non-linearity appears and peak load, which further illustrates the importance of infill walls on structural performance.

The failure patterns of models Wt062, Wt122, Wt152

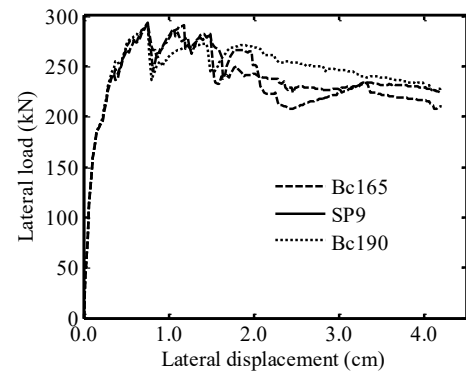


Fig. 16 Lateral load-lateral displacement curves for masonry-infilled RC frame models with different widths of columns

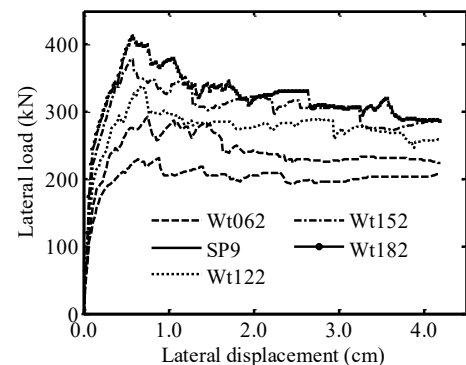


Fig. 17 Lateral load-lateral displacement curves for masonry-infilled RC frame models with different thickness of infill panels



and Wt182 at the lateral displacement of 2.0 cm are shown in Fig. 18. Model Wt062 has a weak filling wall, and its failure pattern is similar to that of specimen 8. A large number of slipping cracks are observed. The failure pattern of model Wt122 is basically the same as that of model SP9, except that the deformation of columns is larger and the shear failure is slightly serious. Models Wt152 and Wt182 have higher strength of infill walls; therefore, the failure patterns are mainly manifested by the shear slipping along with mortar joints, separation of masonry units, and a diagonal compression strut mechanism is also clearly formed. In addition, due to the gradual strengthening of the infill wall, the damage of frame columns is increased.

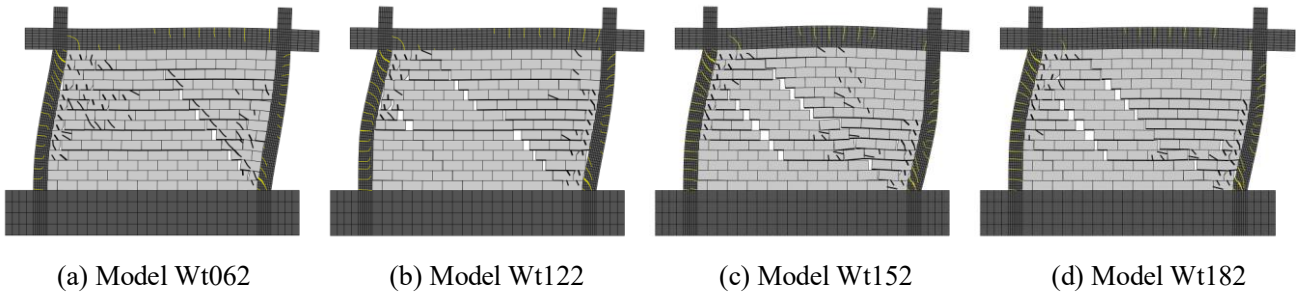


Fig. 18 Failure patterns for masonry-infilled RC frames with different thicknesses of infill panels

3.8 Effect of frictional coefficient in mortar joints

In infill walls, the frictional coefficient of mortar joints is one of the most important parameters. In this section, four additional models are established for numerical analyses by adjusting frictional coefficient of mortar joints. The initial frictional coefficient of horizontal mortar joints in model SP9 is 1.0, and four models are named U0.5, U0.75, U1.25, and U1.5 according to their initial frictional coefficients.

The lateral load-lateral displacement curves of five models are shown in Fig. 19. The initial stiffness values are basically the same, which shows that the frictional coefficient of mortar joints has little effect on the initial stiffness. As the load increases, the frame and the infill wall are gradually separated, the slipping of mortar joints is gradually increased, and the differences between curves gradually appear. The frictional coefficient has a large effect on the peak load, which is mainly because the change in the frictional coefficient directly affects the lateral resistance of the infill wall. It is noticed that models U1.25 and U1.5 have similar peak load, which shows that the increase of frictional coefficient does not constantly increase the bearing capacity. Analyzing the reason, it is because that when the frictional coefficient increases to a certain degree, the bearing capacity is determined by compressive damage due to insufficient strength of masonry units, rather than slipping of mortar joints.

The failure patterns at the lateral displacement of 2.0cm is shown in Fig. 20. As the frictional coefficient of mortar joints increases, the failure pattern of infill walls has changed greatly, from large horizontal slipping failure to diagonal compressive cracking failure. When the frictional coefficient is small (such as model U0.5), the failure of the infill wall is mainly manifested as a large amount of sliding cracks along horizontal mortar joints; as the frictional coefficient increases (such as models U0.75 and SP9), the damage of infill walls gradually changes to the combination of horizontal slipping and stepped inclined cracks; when the frictional coefficient is large (such as models U1.25 and U1.5), the infill wall undergoes the severe diagonal compressive failure. The diagonal failure of the infill wall is mainly determined by its compressive strength, which further confirms the similarity of two models in bearing capacity. In addition, with the increase of frictional coefficient, the increase of lateral resistance of the infill wall also leads to a more severe shear failure of frame columns.

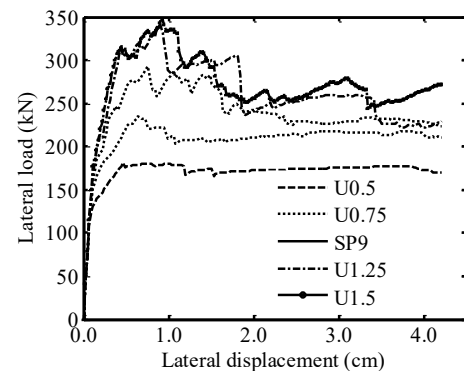


Fig. 19 Lateral load-lateral displacement curves for masonry-infilled RC frame models with different frictional coefficients

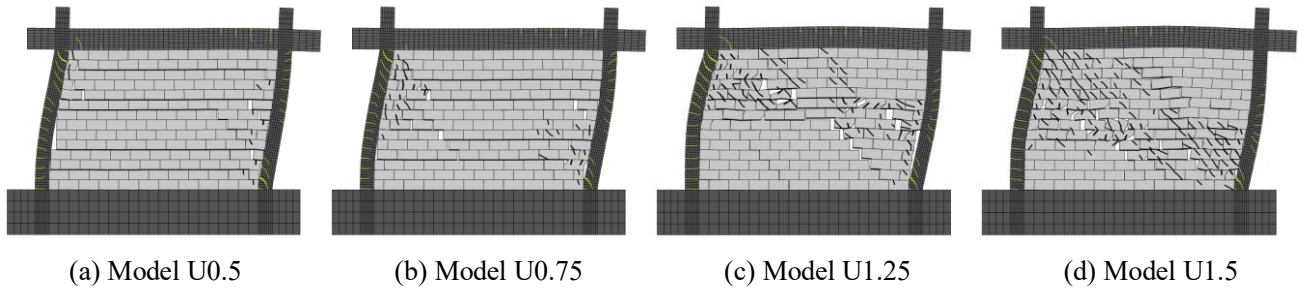


Fig. 20 Failure patterns for masonry-infilled RC frames with different frictional coefficients

3.9 Effect of beam section

Compared with frame columns and infill walls, it is generally believed that frame beams have less impact on structural performance. Frame beams mainly affect distribution of vertical loads and deformation constraint on frame columns and infill walls. Therefore, in this section, the effect of frame beam on structural performance is analyzed by adjusting the height of beam section. According to the ratio of beam section height to that of model SP9, four additional models are named Hb0.5, Hb0.75, Hb1.5, and Hb2.0.

The lateral load-lateral displacement curves of five models are shown in Fig. 21. It can be seen that except for model Hb0.5, beam section height has little effect on the overall trend of curves, including the initial stiffness, peak load, lateral displacement at the peak load and post peak response. For model Hb0.5, the initial stiffness and peak load are similar with that of other models, however, the peak load is smaller and the corresponding lateral displacement at the peak load is larger. This may be because the height of frame beam is reduced too much, the performance is significantly reduced in terms of stiffness and strength, and the constraint to the infill wall is weakened.

The failure patterns for these model are not plotted for conciseness, which are similar except for model HB0.5. In model Hb0.5, because frame beam is severely weakened, the frame deformation is mainly reflected in the deformation of frame beam. Meanwhile, the rotation restriction on frame column is reduced, therefore, the inflection point at the top of windward column is shifted downward. Due to the lack of constraints of the frame on the infill wall, the deformation of the infill wall is larger. In other models, the most obvious difference in damage is the damage of the beam itself. Although the deformation of the infill wall is affected, the section height of frame beam has little effect on the failure pattern of the infill wall. For the failure of frame columns, the effect for models Hb0.75, Hb1.5 and Hb2.0 are also small.

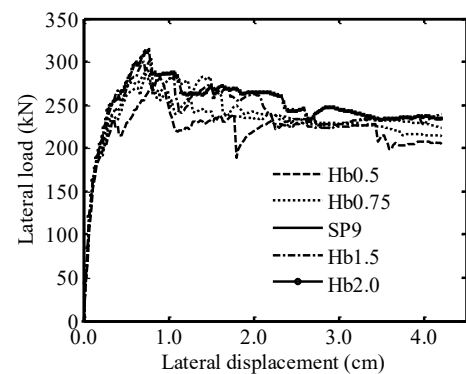


Fig. 21 Lateral load-lateral displacement curves for masonry-infilled RC frame models with different heights of beams

4. Conclusion

A parametric study is performed in this paper to reveal the effect of geometric parameters, design details and material properties on structural performance of masonry-infilled RC frames by using a validated finite element modeling. The initial stiffness is mainly affected by aspect ratio of the infill wall and thickness of the infill wall. The section height of column and beam and the reinforcement arrangement have a slight effect on the initial stiffness; while the vertical load and its distribution have little effect. It illustrates that the initial stiffness should be mainly determined by the stiffness of the infill wall. Furthermore, the bearing capacity of infilled RC frames is mainly affected by aspect ratio of the infill wall, vertical load, vertical load distribution, and frictional coefficient of mortar joints. These parameters mainly affect the frictional force of the infill wall, which finally determines the bearing capacity. The section height of frame column and beam and longitudinal reinforcement also have a certain effect on the bearing capacity. In addition, the section



width of frame column and transverse reinforcement have little effect on the stiffness and bearing capacity, however, these parameters improve the ductility. These important findings can be used to develop simplified analytical procedure for the assessment of seismic performance of infilled RC frame structures.

5. Acknowledgements

This investigation is supported by Scientific Research Fund of Institute of Engineering Mechanics, China Earthquake Administration (Nos. 2018B07, 2016A01, 2018D15), the National Nature Science Foundation of China (Nos. 51808478, 51908484). These supports are greatly appreciated.

6. Copyrights

17WCEE-IAEE 2020 reserves the copyright for the published proceedings. Authors will have the right to use content of the published paper in part or in full for their own work. Authors who use previously published data and illustrations must acknowledge the source in the figure captions.

7. References

- [1] Fiorato A E, Sozen M A, Gamble W L (1970): An Investigation of the Interaction of Reinforced Concrete Frames with Masonry Filler Walls. *Urbana: Technical Report No. IULU-ENG 70-100, Dept. of Civil Engineering, University of Illinois, Urbana, Champaign.*
- [2] Klingner R E, Bertero V V (1978): Earthquake Resistance of Infilled Frames. *(ASCE) Journal of the Structural Division*, 104: 973–989.
- [3] Zarnic R, Tomazevic M (1988): An Experimentally Obtained Method for Evaluation of the Behavior of Masonry Infilled RC Frames. *Proceedings of the 9th World Conference on Earthquake Engineering*, 163-168, Tokyo and Kyoto, Japan.
- [4] Mehrabi A B, Shing P B, Schuller M P, Noland J L (1994): Performance of Masonry-infilled R/C Frames under In-plane Lateral Loads. *Report CU/SR-94/6, Department of Civil, Environmental & Architectural Engineering, University of Colorado, Boulder, USA.*
- [5] Mosalam K M, White R N, Gergely P (1997): Static Response of Infilled Frames using Quasistatic Experimentation. *(ASCE) Journal of Structural Engineering*, 123(11): 1462-1469.
- [6] Al-Chaar G, Issa M, Sweeney S (2002): Behavior of Masonry-infilled Nonductile Reinforced Concrete Frames. *(ASCE) Journal of Structural Engineering*, 128(8): 1055-1063.
- [7] Anil Ö, Altin S (2007): An Experimental Study on Reinforced Concrete Partially Infilled Frames. *Engineering Structures*, 29: 449-460.
- [8] Blackard B, Willam K, Mettupalayam S (2009): Experimental Observations of Masonry Infilled RC Frames with Openings. *Thomas TC Hsu Symposium on Shear and Torsion in Concrete Structures*, 199-222, Farmington Hills, Michigan, USA.
- [9] Stavridis A (2009): Analytical and Experimental Study of Seismic Performance of Reinforced Concrete Frames Infilled with Masonry Walls. *Department of Structural Engineering, University of California San Diego, San Diego, USA.*
- [10] Koutromanos I (2011): Numerical Analysis of Masonry-infilled Reinforced Concrete Frames Subjected to Seismic Loads and Experimental Evaluation of Retrofit Techniques. *Department of Structural Engineering, University of California at San Diego, San Diego, USA.*
- [11] Zhai C H, Wang X M, Kong J C, Li S, Xie L L (2017): Numerical Simulation of Masonry-infilled RC Frames Using XFEM. *(ASCE) Journal of Structural Engineering*, 143(10), 04017144-1-14.